Am J Transl Res 2018;10(7):2068-2077
www.ajtr.org /ISSN:1943-8141/AJTR0076764

Original Article

Comparative study of nanostructured carriers of calcium phosphate and magnesium phosphate loaded with SRT1720 for the protection of H_2O_2-induced senescent endothelium

Zhi-Xiao Su[1,2*], Yi-Qin Shi[3*], Zhao-Yang Lu[2], Rui-Lin Li[2], Xue-Lian Wang[2], Bing-Bing Ning[2], Jun-Li Duan[2], Liang-Shi Hao[2], Jun-Hui Duan[4], Yue Li[5], Ying-Jie Zhu[6], Chang-Ning Hao[4], Rui Wang[1]

[1]Shanghai Key Laboratory of New Drug Design, School of Pharmacy, East China University of Science and Technology, Meilong Road 130, Shanghai 200237, China; [2]Clinical Research Unit, Xinhua Hospital, School of Medicine, Shanghai Jiaotong University, Kongjiang Road 1665, Shanghai 200092, China; [3]Department of Nephrology, Zhongshan Hospital, Fudan University, Fenglin Road 180, Shanghai 200032, China; [4]Department of Cardiology, Tenth People's Hospital of Tongji University, Yanchang Road 301, Shanghai 200072, China; [5]Division of Pulmonary and Critical Care Medicine, Department of Medicine, School of Medicine, University of Maryland, 20 Penn Street, HSF-2, Room #S112, Baltimore 21201, MD, USA; [6]State Key Laboratory of High Performance Ceramics and Superfine Microstructure, Shanghai Institute of Ceramics, Chinese Academy of Sciences, Shanghai 200050, China. [*]Equal contributors.

Received March 26, 2018; Accepted June 23, 2018; Epub July 15, 2018; Published July 30, 2018

Abstract: Nanostructured calcium phosphate (CaP) and magnesium phosphate (MgP) are promising for the application as the nanocarriers in drug delivery. However, the difference between CaP and MgP nanocarriers in drug delivery is rarely investigated. In this work, we comparatively investigated nanostructured CaP, MgP and calcium magnesium phosphate (CMP) for the delivery of SRT1720, which is a silent information regulator (SIRT1) specific activator with pro-angiogenic and anti-aging properties in response to hydrogen peroxide (H_2O_2)-induced endothelial senescence. The protection of SRT1720-loaded CaP nanospheres, MgP nanosheets and CMP microspheres on the H_2O_2-induced senescent endothelium was examined by using human umbilical vein endothelial cells (HUVECs), demonstrating the improved cell viability, anti-aging, tube formation and migration. In addition, the SRT1720-loaded CaP nanospheres, MgP nanosheets and CMP microspheres can rescue the impaired angiogenic potential of HUVECs via activation of Akt/eNOS/VEGF pathway. The SRT1720-loaded MgP nanosheets and CMP microspheres have a similar protective effect compared with the pure SRT1720, while the SRT1720-loaded CaP nanospheres decrease the protective capability of SRT1720. These results lead us to figure out both MgP nanosheets and CMP microspheres are suitable and effective delivery for SRT1720 and this system can be further applied *in vivo* treatment.

Keywords: Nanostucture, calcium phosphate, magnesium phosphate, SRT1720, endothelial cell senescence

Introduction

The mortality of cardiovascular disease (CVD) is higher than others all over the world. One of the primary risk factor of CVD is aging. Aging is dramatically related to vascular cell deterioration which leads to the disruption of normal vascular tension and vascular diseases [1, 2]. The vascular tension, integrity and remodeling are mainly dependent on vascular endothelial cells (VECs) regulation to keep the vascular homeostasis [3]. Aging would cause endothelial senescence and augment regeneration ability decrease, which has been discovered in patients with atherosclerosis, diabetes, hyperlipidemia, hypertension, obesity, and aging [4-8].

Sirtuin belongs to histone deacetylases family with homological molecular structure to saccharomyces cerevisiae silent information regulator 2 (Sir2) that requires nicotinamide-adenine dinucleotide as a cofactor for the deacetylation reaction. The sirtuin mediated deacetylases are proved to be regulated by oxidative

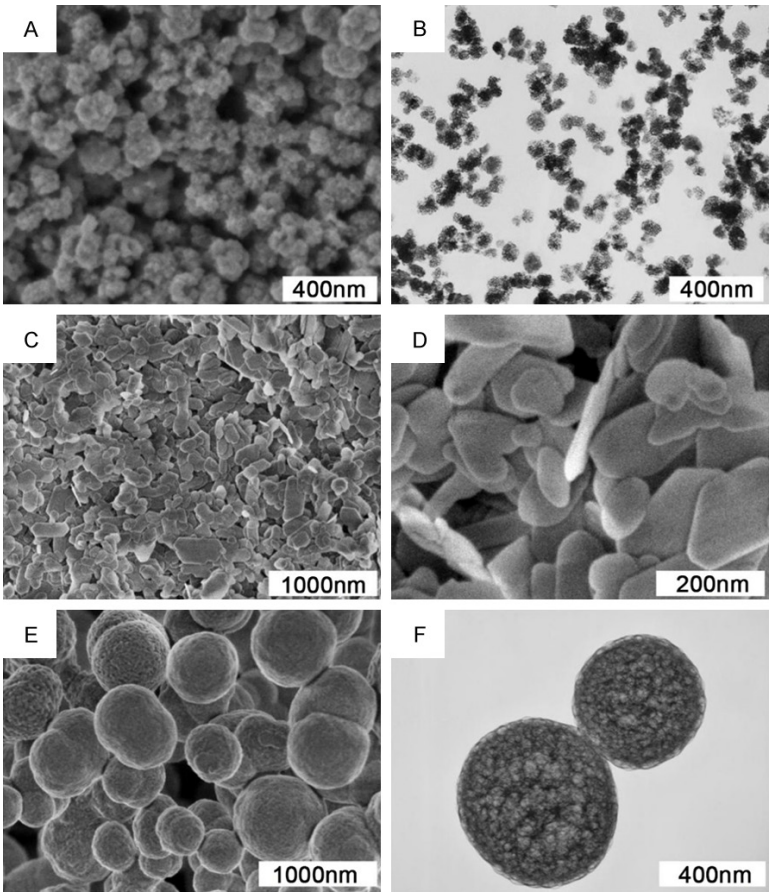

Figure 1. Characterization of nanostructured CaP, MgP and CMP. SEM (A and C-E) and TEM (B and F) micrographs of CaP nanospheres (A and B), MgP nanosheets (C and D) and CMP microspheres (E and F).

stress, metabolism and microenvironment [9]. In mammals, there are seven different sirtuins. Among the seven human sirtuins, Sirtuin-1 (SIRT1) plays the most critical roles during the processes of cell senescence, organism longevity, stress resistance, gene silencing, apoptosis and inflammation [10-12]. The expression of SIRT1 is extremely high in VECs and regulates the function of VECs [13]. Thus, alterations in endothelial SIRT1 expression would affect normal vascular endothelial function and vascular physiology. The protective effects of SIRT1 in cardiovascular diseases have been emphasized in recent studies [14, 15]. SRT-1720, a new synthetic small molecule, has been confirmed the specific activation of SIRT1 [16]. In our previous study, we demonstrated the anti-aging and anti-apoptotic beneficial of SRT1720 and confirmed that SRT1720 rescued the impaired angiogenic potential of HUVECs via activation of Akt/eNOS/VEGF signaling pathway [17].

In further clinical practice, SRT1720 need to be co-administered with other substances to maximize the therapeutic effects while minimizing the possible side effects. Over the past three decades, the use of nanoscale carriers to achieving targeted delivery has been focused. Nanostructured calcium phosphate (CaP) and magnesium phosphate (MgP) are promising nanocarriers for drug delivery owing to their excellent biocompatibility, high drug loading capacity and pH-sensitive drug release property [18-24]. Usually, nanostructured CaP or MgP was investigated independently for drug delivery. The difference in drug delivery between CaP and MgP nanocarriers was rarely reported. Herein, we comparatively investigate nanostructured CaP, MgP and calcium magnesium phosphate (CMP) for the delivery of SRT1720, and the protection of SRT-1720-loaded CaP, MgP and CMP nanostructured carriers for the H_2O_2-induced senescent endothelium. We would figure out the suitable nanoscale carriers for SRT1720 to achieve anti-aging and anti-apoptotic effects and uncover the underlying molecular mechanisms.

Materials and methods

Preparation of CaP nanospheres

CaP nanospheres were synthesized according to our previous report [25]. In brief, 0.110 g of adenosine 5'-triphosphate disodium salt (ATP) was added into 30 mL of $CaCl_2$ (111 mg) solution and the pH value was adjusted to 9 using 1 M NaOH, then 10 mL of Na_2CO_3 (106 mg) solution was added dropwise to the above solution under magnetic stirring, and the pH value was maintained at 9. The resulting suspension was stirred at room temperature for 1 h, loaded into a 60 mL autoclave, sealed, microwave-heated in a microwave oven (MDS-6, Sineo, China) to

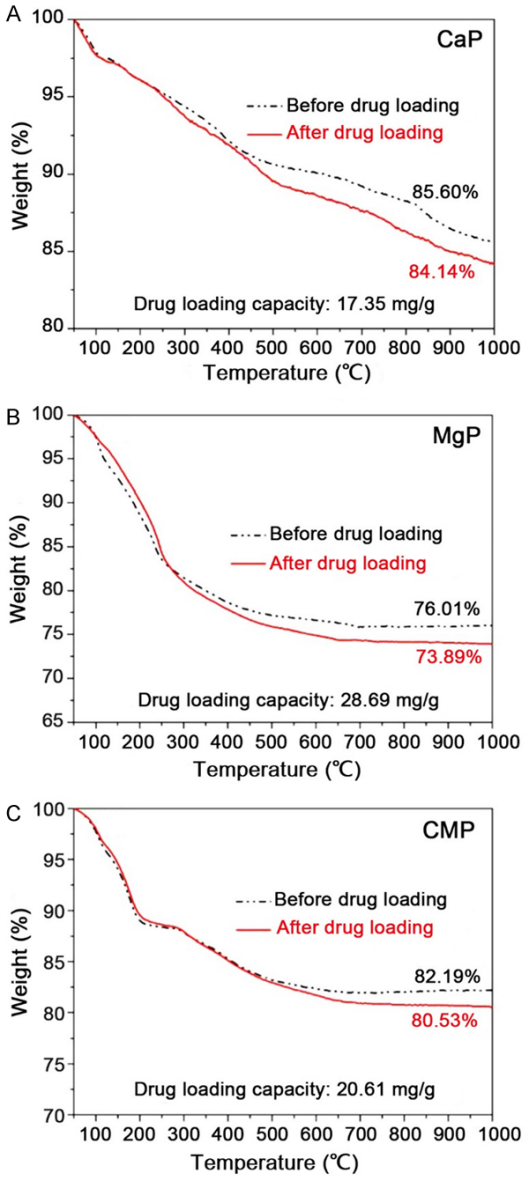

Figure 2. TG curves of the as-prepared CaP nanospheres (A), MgP nanosheets (B), and CMP microspheres (C) before and after drug loading.

180°C, maintained at this temperature for 10 min, and then cooled naturally to room temperature. The product was separated by centrifugation, washed with deionized water and ethanol several times, and dried at 60°C for 24 h.

Preparation of MgP nanosheets

MgP nanosheets were synthesized according to our previous report [24]. 12 mL of $MgCl_2 \cdot 6H_2O$ (244 mg) solution and 8 mL of $NaH_2PO_4 \cdot 2H_2O$ (125 mg) solution were added dropwise to 20 mL of deionized water under magnetic stirring at room temperature while the pH value was maintained at pH 10 using 1 M aqueous solution of NaOH. The resulting suspension was loaded into an autoclave (60 mL), sealed, heated in a microwave oven (MDS-6, Sineo, China) to 120°C, and maintained at this temperature for 10 min. After cooling to room temperature, the product was separated by centrifugation, washed with deionized water and ethanol several times, and dried at 60°C for 24 h.

Preparation of CMP microspheres

CMP microspheres were synthesized according to our previous report [26]. 3 mL of $CaCl_2$ (100 mM), 7 mL of $MgCl_2 \cdot 6H_2O$ (100 mM) and 10 mL of creatine phosphate disodium salt tetrahydrate (60 mM) were added dropwise to 20 mL of deionized water under magnetic stirring at room temperature. The resulting suspension was loaded into an autoclave (60 mL), sealed, heated in a microwave oven (MDS-6, Sineo, China) to 150°C, and maintained at this temperature for 10 min. After cooling to room temperature, the product was separated by centrifugation, washed with deionized water and ethanol several times, and dried at 60°C for 24 h.

Drug loading

Drug loading experiments were performed as follows: dried powder of CaP nanospheres (120 mg), MgP nanosheets (120 mg) or CMP microspheres (120 mg) was dispersed into a solution of ethanol (10 mL) with a SRT1720 concentration of 20 mg mL^{-1}. The suspension was shaken in a sealed vessel at 37°C for 24 h, followed by centrifugation, and then dried to obtain the drug-loaded CaP, MgP and CMP [27].

Characterization

Scanning electron microscopy (SEM) images were recorded with a field-emission scanning electron microscope (FEI Magellan 400, USA). The thermogravimetric (TG) curves were measured on a STA 409/PC simultaneous thermal analyzer (Netzsch, Germany) with a heating rate of 10°C min^{-1} in flowing air.

Cell culture

Human umbilical vein endothelial cells (HUVECs), obtained from the American Type Culture Collection (ATCC, Cat. CRL1730), were mainta-

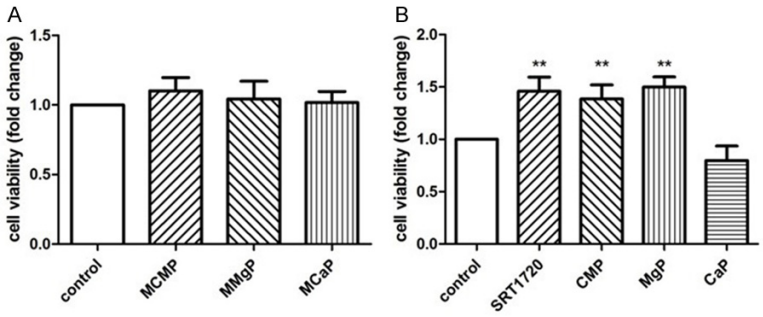

Figure 3. Nanometer materials augmented cell viability of HUVECs. A. HUVECs were pretreated with 1 mM different nanometer material for 24 hours. The proliferation was analyzed by Cell Count Kit-8 (CCK-8) as indicated. B. HUVECs were pretreated with 10 μM SRT1720 and the different microspheres contained 10 μM SRT1720 for 24 hours. The proliferation was analyzed by Cell Count Kit-8 (CCK-8) as indicated. Values are mean ± SEM; n = 4, *means $P<0.05$, **means $P<0.01$. One-way ANOVA (Bonferroni post hoc test) was used.

ined in a humidified atmosphere of 95% air and 5% CO_2 at 37°C. Cells were cultured in Dulbecco's Modified Eagle Medium (DMEM, low glucose) with 10% (v/v) fetal bovine serum (FBS). HUVECs in passages 2-4 were used in this study. According to our previous study, we found that H_2O_2 effectively induced HUVECs senescence following a dose-dependent manner and 300 μM of H_2O_2 displayed a maximum anti-angiogenic effect followed by remarkable endothelial dysfunction. Meanwhile, SRT1720 achieved the maximum efforts at optimum concentration of 10 μM [17]. This time, HUVECs were treated with 300 μM of H_2O_2 (Sigma, St. Louis, MO) for 4 hours to induce cell senescence. For analyzing the anti-aging effect of SRT1720 (Sellect, Shanghai, China), HUVECs were pretreated with 10 μM (final concentration) SRT1720 or SRT1720-loaded CaP, MgP and CMP nanostructured carriers for 24 hours before H_2O_2 administration. Supernatant and cell lysates were collected for biological analysis.

CCK-8 assay

WST-8 Cell Counting Kit-8 (CCK-8 kit, Beyotime) was used to analyze cell growth. After treated with 1 mM different nanometer materials (MCaP, MMgP, MCMP) or SRT1720 and SRT1720-loaded CaP, MgP and CMP nanostructured carriers (the final concentration of SRT1720 was 10 μM), HUVECs (2×10^4/mL) were seeded on 96-well plates with 100 μL DMEM (with 10% FBS) and incubated at 37°C. After 24 hours 10 μL CCK-8 solution was added and incubated at 37°C for 2 hours. The absorbance of the reactive system was measured at 450 nm wavelength.

Galactosidase (β-gal) staining

After treated with 10 μM pure SRT1720 or SRT1720-loaded CaP, MgP and CMP nanostructured carriers for 24 hours, HUVECs were treated with or without 300 μM H_2O_2 for 4 hours. Then the cells washed twice with PBS and stained by β-Galactosidase Staining Kit (Beyotime, Shanghai, China) for SA-β-gal activity analyses. The number of blue cells (×100 magnification) was counted in 5 random fields to determine the percentage of SA-β-gal positive cells [28].

Transwell migration assay

24-well Boyden Transwell chambers (Corning, Cambridge, MA) with 6.5-mm-diameter polycarbonate filters (8-μm pore size) were employed to determine cells migration. Briefly, 600 μL DMEM (with 10% FBS) was added into the lower compartment. HUVECs (3×10^5/mL) treated with H_2O_2 and pure SRT1720 or SRT1720-loaded CaP, MgP and CMP nanostructured carriers were seeded in upper compartment of the transwell chambers in 100 μL serum-free Medium. 12 hours later, the cells that migrated to the underside were fixed with cold 4% paraformaldehyde and stained with 0.1% crystal violet. Stained cells were counted in 5 random fields using light microscopy (×100 magnification).

Tube formation assay

The tube formation assay was performed as described previously [29]. In brief, HUVECs (5×10^5/mL) treated with or without H_2O_2 together with pure SRT1720 or SRT1720-loaded CaP, MgP and CMP suspended by 50 μL DMEM (with 10% FBS) were reseeded into Matrigel (BD Biosciences) coated 96-well dishes, and exposed to their original mediators. After 6-8 hours' incubation, graphs were captured with a

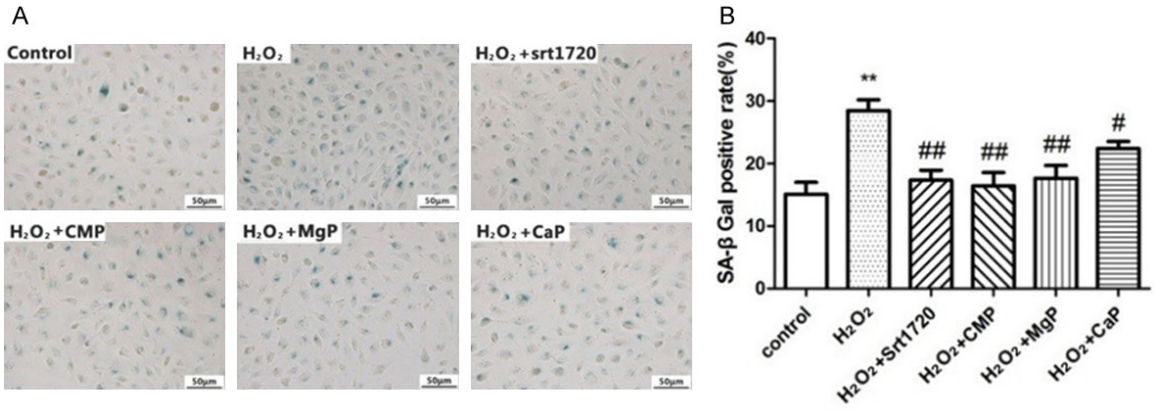

Figure 4. SRT1720 augmented cell viability of HUVECs. HUVECs were pretreated with or without 10 μM SRT1720 and the different microsphere contained 10 μM SRT1720 for 24 hours, followed by 300 μM H_2O_2 or PBS for additional 4 hours. (A) SA-β-gal staining was performed and senescent cells were stained with blue color, (B) The ratio of SA-β-gal positive cells was calculated per group. Values are mean ± SEM; n = 4, *means P<0.05, **means P<0.01, vs. control group, #means P<0.05, ##means P<0.01, vs. H_2O_2 group. Scale bar indicated 50 μm. One-way ANOVA (Bonferroni post hoc test) was used.

fluorescent microscope (IX-71; Olympus, Tokyo, Japan) with 12.8 M pixel recording digital color cooled camera (DP72; Olympus). Each experiment was repeated 4 times. The images of tube morphology were taken and tube lengths were calculated and represented as fold of control under ×100 magnification.

Western blotting

Cell lysates of HUVEC treated with H_2O_2 and pure SRT1720 or SRT1720-loaded CaP, MgP and CMP nanostructured carriers. Equal amounts of total protein from the cell lysates of HUVECs were resolved in SDS 10% polyacrylamide gel and transferred to nitrocellulose membranes for Western blotting as described previously [30, 31]. The primary antibodies were follows, anti-eNOS (1:1000, Sigma, St. Louis, MO), anti-VEGF (1:1000, Proteintech, Chicago, IL), anti-phosphor-Akt (p-Akt) and anti-GAPDH (1:1000, Cell Signaling Technology, Beverly, MA). Positive signals were visualized with a FluorChem E data system (Cell Biosciences, Santa Clara, CA) and quantified by densitometry using Quantity One 4.52 (Bio-Rad, Hercules, CA). Blots were reprobed with GAPDH to confirm equal loading of cell lysate proteins.

Statistical analysis

Data were expressed as mean ± standard error of the mean (SEM). One-way ANOVA analysis of variance with the post-hoc Bonferroni test was applied for multiple comparisons. Statistical analysis was performed in SPSS software version 17.0 (SPSS Inc., Chicago, IL, USA). All experiments were repeated at least four times. *P* values <0.05 were considered significant.

Results

Characterization of nanostructured CaP, MgP and CMP

The morphology of the prepared CaP sample was observed by SEM and TEM. From the SEM (**Figure 1A**) and TEM (**Figure 1B**) micrographs, one can see that the CaP sample was composed of CaP nanospheres, which formed by the self-assembly of CaP nanopaticles. According to our previous study [25], the crystal phase of the as-prepared CaP nanospheres was carbonated hydroxyapatite. The SEM micrographs (**Figure 1C** and **1D**) of the as-prepared MgP sample indicate that the MgP sample was composed of nanosheets, and the crystal phase of the as-prepared MgP nanosheets was magnesium phosphate hydrate ($Mg_3(PO_4)_2{\cdot}5H_2O$) [24]. The as-prepared CMP sample was composed of microspheres constructed by self-assembled nanoparticles, and the crystal phase was amorphous calcium magnesium phosphate [26].

The TG curves of the as-prepared samples are shown in **Figure 2**. The weight loss of the CaP nanospheres (**Figure 2A**) was approximately 14.40%, while the weight loss of drug-loaded

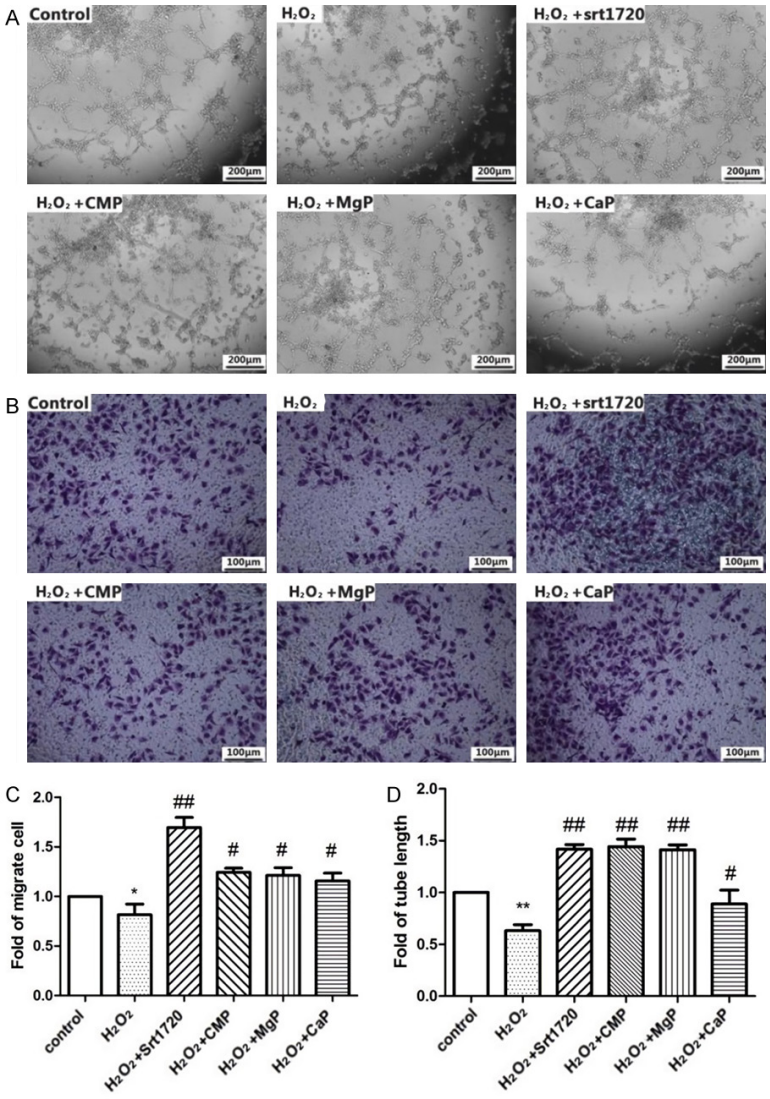

Figure 5. SRT1720 augmented cell viability of HUVECs. HUVECs were pretreated with or without 10 μM SRT1720 and the different SRT1720 microsphere for 24 hours, followed by 300 μM H_2O_2 or PBS for additional 4 hours. A. Representative images of tube formation and quantitative analysis of tube length were represented as fold of control. B. Migrated cells were stained and quantitative analysis of migrated cells was represented as fold of control. C. The statistical graph of migrate cell. D. The statistical graph of tube length. Values are mean ± SEM; n = 4, **means P<0.01, vs. control, #means P<0.05, ##means P<0.01, vs. H_2O_2 group. One-way ANOVA (Bonferroni post hoc test) was used.

CaP was 15.86%, thus the drug loading capacity of the CaP was about 17.35 mg g^{-1} (milligram drug per gram carrier). For the MgP nanosheets (**Figure 2B**), the weight loss of MgP was approximately 23.99%, while the weight loss of drug-loaded MgP was 26.11%, and the drug loading capacity was about 28.69 mg g^{-1}. For the CMP microspheres, the weight loss of CMP before and after drug loading was 17.81% and 19.47%, respectively, thus the drug loading capacity was about 20.61 mg g^{-1}.

The effects of nanometer materials and SRT1720-loaded nanostructured carriers on normal HUVECs

The CCK-8 assay shows that the viability of HUVECs treated with three different nanometer materials has no significant difference with the control group (**Figure 3A**). The result indicated that the nanometer materials themselves didn't influence the viability of HUVECs and safe for application. Then, we analyze the function of SRT1720 and SRT1720-loaded nanostructured carriers on normal HUVECs. All the final concentration of SRT1720 is 10 μM. As shown in **Figure 3B**, SRT1720-loaded CMP and MgP, similar as pure SRT1720, significantly ameliorate the viability of HUVECs to compare with control group and SRT1720-loaded CaP group. There was almost no difference between SRT1720-loaded CaP groups and control ones.

The protective effects of SRT1720-loaded nanometer materials on H_2O_2-treated HUVECs

In previous study, we confirmed that SRT1720 rescued the senescent HUVECs on the cell apoptosis, tube formation, migration and cell proliferation [17]. In present study, we compared the effect of SRT1720 loaded nanostructured carriers and pure SRT1720. The result indicated that the protective effect of SRT1720-loaded CMP and MgP was similar to pure SRT1720. SRT1720-loaded CaP could also rescue the senescent HUVECs but less effective (**Figure 4A**, **4B**). We also investigated the effect of three SRT1720-loaded-microspheres on HUVECs tube formation. The three SRT1720-loaded nanostructured carriers significantly enhanced the tube formation which was similar as pure SRT1720. The effect of SRT1720-load-

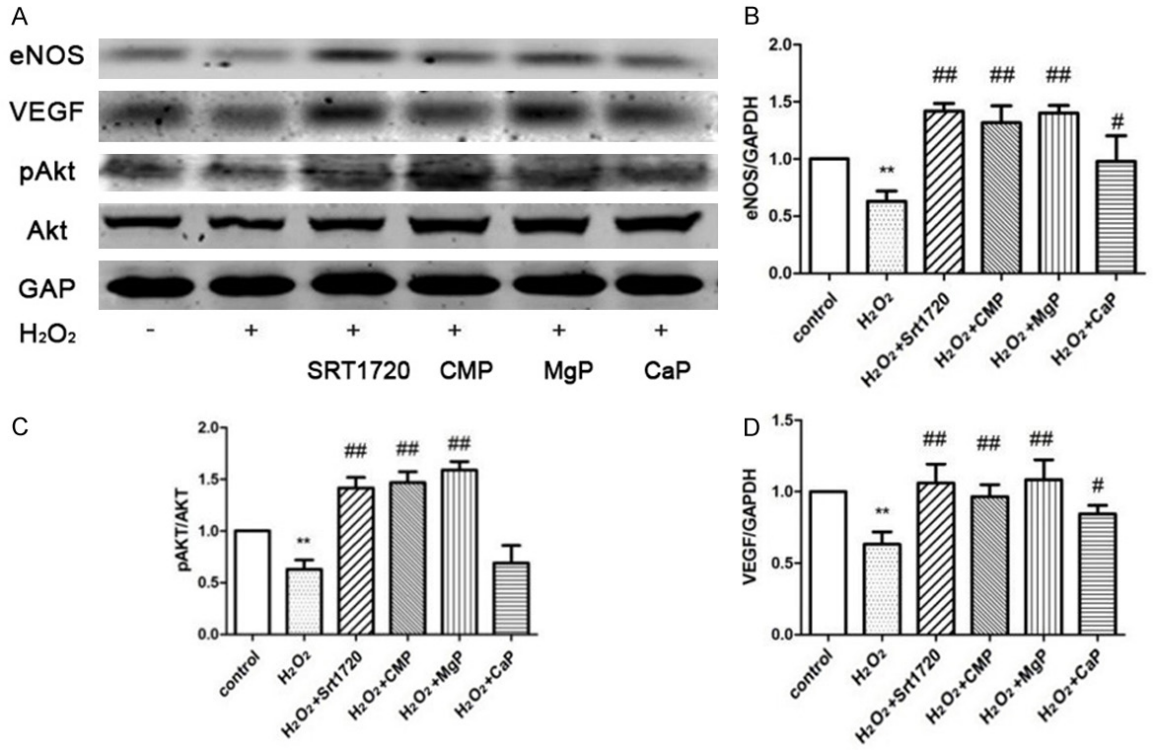

Figure 6. SRT1720 augmented cell viability of HUVECs. HUVECs were pretreated with or without 10 μM SRT1720 and the different SRT1720 microsphere for 24 hours, followed by 300 μM H_2O_2 or PBS for additional 4 hours. The protein expressions of eNOS, VEGF, pAkt, and Akt in HUVECs were examined by Western blotting, data were represented as fold of control. Values are mean ± SEM; n = 4, *means P<0.05, **means P<0.01, vs. control group, #means P<0.05, ##means P<0.01, vs. H_2O_2 group. One-way ANOVA (Bonferroni post hoc test) was used.

ed CaP was weaker than that of others (**Figure 5A**, **5C**). For migration assay, we found that although SRT1720-loaded nanostructured carriers can improve HUVECs migration significantly than non-treated group, the effect was not as good as pure SRT1720 (**Figure 5B**, **5D**).

SRT1720 and SRT1720-loaded nanometer particles showed similar effects on angiogenic factors in H_2O_2-treated HUVECs

HUVECs were pre-treated with or without 10 μM SRT1720 or SRT1720-loaded nanostructured carriers for 24 hours, followed by 300 μM H_2O_2 or PBS for 4 hours and then continue incubated for additional 24 hours. We found that pure SRT1720 could significantly activate sirt1 expression and increase angiogenic factors (eNOS, VEGF and pAkt/Akt) level in H_2O_2-induced senescent HUVECs. The result well matched our previous study [17]. The effect of SRT1720-loaded CMP and MgP were similar as pure SRT1720 (**Figure 6**), while the SRT1720-loaded CaP nanospheres decrease the protective effect of SRT1720.

Discussion

Calcium and magnesium are both important elements of human body. They play important roles in regulating various life activities of human beings. They are widely distributed in hard tissues such as bones and teeth in the form of phosphate. Therefore, the synthetic calcium/magnesium phosphate nanomaterials have good biocompatibility and are widely used in biomedicine and other fields [32, 33]. Therefore, SRT1720-loaded CaP nanospheres, MgP nanosheets and CMP microspheres can be further applied to the organism.

In our study, 300 μM of H_2O_2 induced a significant anti-angiogenic effect of HUVECs and remarkable endothelial dysfunction. This cellular model was used to evaluate the ability of different SRT1720-loaded nano-carriers to protect HUVECs. As the carriers of SRT1720, the

drug loading capacity of CaP, MgP and CMP are similar. Nanomaterials CaP, MgP and CMP didn't influence the viability of HUVECs and safe for application. However, the SRT1720-loaded nanostructured carriers showed different effects on normal HUVECs and H_2O_2-treated HUVECs in several assays. The pore size and other characteristics of the nanomaterials maybe cause different drug release capability which influenced the results [34, 35]. The protect ability of SRT1720-loaded CaP was weaker than others.

In summary, we comparatively investigate nanostructured CaP, MgP and CMP for the delivery of SRT1720, and the protection of SRT1720-loaded CaP, MgP and CMP nanostructured carriers for the H_2O_2-induced senescent endothelium. In comparison with pure SRT1720, SRT1720-loaded MgP and CMP show the similar effects on promoting cell proliferation, migration and tube formation, while the capacity of SRT1720-loade CaP was weaker. To further investigate the underline mechanism, we found that SRT1720-loaded CaP nanospheres, MgP nanosheets and CMP microspheres can rescue the impaired angiogenic potential of HUVECs via activating Akt/eNOS/VEGF pathway. These results suggested that MgP nanosheets and CMP microspheres should be the most suitable carriers for SRT1720. We'll further apply this system *in vivo* study.

Acknowledgements

This work was supported by the the Opening Project of Shanghai Key Laboratory of New Durg Design (17DZ2271000), China National Natural Science Foundation (11374213, 11574210, 81500523 and 81500372) and Funding for Clinical Trial of Xinhua Hospital (DJL).

Disclosure of conflict of interest

None.

Address correspondence to: Dr. Rui Wang, Shanghai Key Laboratory of New Drug Design, School of Pharmacy, East China University of Science and Technology, Meilong Road 130, Shanghai 200237, China. E-mail: ruiwang@ecust.edu.cn; Dr. Chang-Ning Hao, Department of Cardiology, Tenth People's Hospital of Tongji University, Yanchang Road 301, Shanghai 200072, China. E-mail: gilberthaocn@gmail.com; Dr. Ying-Jie Zhu, State Key Laboratory of High Performance Ceramics and Superfine Microstructure, Shanghai Institute of Ceramics, Chinese Academy of Sciences, Shanghai 200050, China. E-mail: y.j.zhu@mail.sic.ac.cn; Dr. Yue Li, Division of Pulmonary and Critical Care Medicine, Department of Medicine, School of Medicine, University of Maryland, 20 Penn Street, HSF-2, Room #S112, Baltimore 21201, MD, USA. E-mail: YueLi@som.umaryland.edu

References

[1] Head T, Daunert S and Goldschmidt-Clermont PJ. The aging risk and atherosclerosis: a fresh look at arterial homeostasis. Front Genet 2017; 8: 216.

[2] Paneni F, Canestro CD, Libby P, Luscher TF and Camici GG. The aging cardiovascular system understanding it at the cellular and clinical levels. J Am Coll Cardiol 2017; 69: 1952-1967.

[3] Behrendt D and Ganz P. Endothelial function: from vascular biology to clinical applications. Am J Cardiol 2002; 90: 40L-48L.

[4] Chen CA, Wang TY, Varadharaj S, Reyes LA, Hemann C, Talukder MA, Chen YR, Druhan LJ and Zweier JL. S-glutathionylation uncouples eNOS and regulates its cellular and vascular function. Nature 2010; 468: 1115-8.

[5] Minamino T, Miyauchi H, Yoshida T, Ishida Y, Yoshida H and Komuro I. Endothelial cell senescence in human atherosclerosis-role of telomere in endothelial dysfunction. Circulation 2002; 105: 1541-1544.

[6] Yang Y, Duan W, Liang Z, Yi W, Yan J, Wang N, Li Y, Chen W, Yu S, Jin Z and Yi D. Curcumin attenuates endothelial cell oxidative stress injury through Notch signaling inhibition. Cell Signal 2013; 25: 615-629.

[7] Seals DR, Jablonski KL and Donato AJ. Aging and vascular endothelial function in humans. Clin Sci (Lond) 2011; 120: 357-375.

[8] Lu ZY, Li RL, Zhou HS, Huang JJ, Su ZX, Qi J, Zhang L, Li Y, Shi YQ, Hao CN and Duan JL. Therapeutic ultrasound reverses peripheral ischemia in type 2 diabetic mice through PI3K-Akt-eNOS pathway. Am J Transl Res 2016; 8: 3666-3677.

[9] Houtkooper RH, Pirinen E and Auwerx J. Sirtuins as regulators of metabolism and healthspan. Nat Rev Mol Cell Biol 2012; 13: 225-238.

[10] Yao H, Chung S, Hwang JW, Rajendrasozhan S, Sundar IK, Dean DA, McBurney MW, Guarente L, Gu W, Ronty M, Kinnula VL and Rahman I. SIRT1 protects against emphysema via FOXO3-mediated reduction of premature senescence in mice. J Clin Invest 2012; 122: 2032-2045.

[11] Jose Zarzuelo M, Lopez-Sepulveda R, Sanchez M, Romero M, Gomez-Guzman M, Ungvary Z, Perez-Vizcaino F, Jimenez R and Duarte J. SI-

RT1 inhibits NADPH oxidase activation and protects endothelial function in the rat aorta: implications for vascular aging. Biochem Pharmacol 2013; 85: 1288-1296.
[12] Rahman I, Kinnula VL, Gorbunova V and Yao H. SIRT1 as a therapeutic target in inflammaging of the pulmonary disease. Prev Med 2012; 54: S20-S28.
[13] Arunachalam G, Yao H, Sundar IK, Caito S and Rahman I. SIRT1 regulates oxidant- and cigarette smoke-induced eNOS acetylation in endothelial cells: role of resveratrol. Biochem Biophys Res Commun 2010; 393: 66-72.
[14] Nadtochiy SM, Redman E, Rahman I and Brookes PS. Lysine deacetylation in ischaemic preconditioning: the role of SIRT1. Cardiovasc Res 2011; 89: 643-649.
[15] Vinciguerra M, Santini MP, Martinez C, Pazienza V, Claycomb WC, Giuliani A and Rosenthal N. mIGF-1/JNK1/SirT1 signaling confers protection against oxidative stress in the heart. Aging Cell 2012; 11: 139-149.
[16] Lin YJ, Zhen YZ, Wei J, Liu B, Yu ZY and Hu G. Effects of Rhein lysinate on H2O2-induced cellular senescence of human umbilical vascular endothelial cells. Acta Pharmacol Sin 2011; 32: 1246-1252.
[17] Li RL, Lu ZY, Huang JJ, Qi J, Hu A, Su ZX, Zhang L, Li Y, Shi YQ, Hao CN and Duan JL. SRT1720, a SIRT1 specific activator, protected H_2O_2-induced senescent endothelium. Am J Transl Res 2016; 8: 2876-2888.
[18] Qi C, Zhu YJ, Zhao XY, Lu BQ, Tang QL, Zhao J and Chen F. Highly stable amorphous calcium phosphate porous nanospheres: microwave-assisted rapid synthesis using ATP as phosphorus source and stabilizer, and their application in anticancer drug delivery. Chemistry 2013; 19: 981-987.
[19] Zhao XY, Zhu YJ, Chen F, Lu BQ, Qi C, Zhao J and Wu J. Calcium phosphate hybrid nanoparticles: self-assembly formation, characterization, and application as an anticancer drug nanocarrier. Chemistry 2013; 8: 1306-1312.
[20] Ding GJ, Zhu YJ, Qi C, Sun TW, Wu J and Chen F. Yolk-shell porous microspheres of calcium phosphate prepared by using calciumL-lactate and adenosine 5'-triphosphate disodium salt: application in protein/drug delivery. Chemistry 2015; 21: 9868-9876.
[21] Qi C, Zhu YJ, Lu BQ, Zhao XY, Zhao J, Chen F and Wu J. Hydroxyapatite hierarchically nanostructured porous hollow microspheres: rapid, sustainable microwave-hydrothermal synthesis by using creatine phosphate as an organic phosphorus source and application in drug delivery and protein adsorption. Chemistry 2013; 19: 5332-5341.
[22] Qi C, Zhu YJ and Chen F. Fructose 1,6-bisphosphate trisodium salt as a new phosphorus source for the rapid microwave synthesis of porous calcium-phosphate microspheres and their application in drug delivery. Chemistry 2013; 8: 88-94.
[23] Bhakta G, Mitra S and Maitra A. DNA encapsulated magnesium and manganous phosphate nanoparticles: potential non-viral vectors for gene delivery. Biomaterials 2005; 26: 2157-2163.
[24] Qi C, Zhu YJ, Lu BQ, Ding GJ, Sun TW, Chen F and Wu J. Microwave-assisted rapid synthesis of magnesium phosphate hydrate nanosheets and their application in drug delivery and protein adsorption. J Mater Chem B 2014; 2: 8576-8586.
[25] Qi C, Zhu YJ and Chen F. Microwave hydrothermal transformation of amorphous calcium carbonate nanospheres and application in protein adsorption. ACS Appl Mater Interfaces 2014; 6: 4310-4320.
[26] Qi C, Zhu YJ, Chen F and Wu J. Porous microspheres of magnesium whitlockite and amorphous calcium magnesium phosphate: microwave-assisted rapid synthesis using creatine phosphate, and application in drug delivery. J Mater Chem B 2015; 3: 7775-7786.
[27] Qi C, Zhu YJ, Lu BQ, Ding GJ, Sun TW, Chen F and Wu J. Microwave-assisted rapid synthesis of magnesium phosphate hydrate nanosheets and their application in drug delivery and protein adsorption. J Mater Chem B 2014; 2: 8576-8586.
[28] Lin XL, Liu Y, Liu M, Hu H, Pan Y, Fan XJ, Hu XM and Zou WW. Inhibition of hydrogen peroxide-induced human umbilical vein endothelial cells aging by allicin depends on sirtuin1 activation. Med Sci Monit 2017; 23: 563-570.
[29] Huang JJ, Shi YQ, Li RL, Hu A, Lu ZY, Weng L, Wang SQ, Han YP, Zhang L, Li B, Hao CN and Duan JL. Angiogenesis effect of therapeutic ultrasound on HUVECs through activation of the PI3K-Akt-eNOS signal pathway. Am J Transl Re 2015; 7: 1106-1115.
[30] Li RL, Huang JJ, Shi YQ, Hu A, Lu ZY, Weng L, Wang SQ, Han YP, Zhang L, Hao CN and Duan JL. Pulsed electromagnetic field improves postnatal neovascularization in response to hindlimb ischemia. Am J Transl Res 2015; 7: 430-444.
[31] Hao C, Huang ZH, Song SW, Shi YQ, Cheng XW, Murohara T, Lu W, Su DF and Duan JL. Arterial baroreflex dysfunction impairs ischemia-induced angiogenesis. J Am Heart Assoc 2014; 3: e000804.
[32] Palmer LC, Newcomb CJ, Kaltz SR, Spoerke ED and Stupp SI. Biomimetic systems for hydroxy-

apatite mineralization inspired by bone and enamel. Chem Rev 2009; 40: 4754-4783.
[33] Dorozhkin SV, Epple M. Biological and medical significance of calcium phosphates. Angew Chem Int Ed Engl 2002; 41: 3130-46.
[34] Xu J, Wu C, Yan PT, Zhang RJ, Yue XQ and Ge SH. Pore characteristics of carbide-derived carbons obtained from carbides with different carbon volume fractions. Microporous and Mesoporous Materials 2014; 198: 74-81.
[35] Qi C, Zhu YJ, Sun TW, Wu J, Chen F. Microwave-assisted hydrothermal rapid synthesis of amorphous calcium phosphate mesoporous microspheres using adenosine 5'-diphosphate and application in pH-responsive drug delivery. Chem Asian J 2015; 10: 2503-2511.